

Fluorescent Nitric Oxide Detection by Copper Complexes Bearing Anthracenyl and Dansyl Fluorophore Ligands

Mi Hee Lim and Stephen J. Lippard*

Department of Chemistry, Massachusetts Institute of Technology, Cambridge, Massachusetts 02139

Received June 4, 2006

Anthracenyl and dansyl fluorophore ligands [AnCH₂pipCS₂K (1), Ds-Hen (2), Ds-HAMP (3), Ds-HAQ (4), and Ds-HAPP (5)] were prepared for coordination to Cu^{II}. Five Cu complexes, [Cu(AnCH₂pipCS₂)₂] (6), [Cu(Ds-en)₂] (7), [Cu(Ds-AMP)₂] (8), [Cu(Ds-AQ)₂] (9), and [Cu(Ds-APP)(OTf)] (10), were synthesized as candidates for detecting nitric oxide (NO) by fluorescence and characterized by X-ray crystallography. A decrease in fluorescence compared to that of the free ligands (1–5) was measured following the formation of the corresponding five Cu^{II} complexes 6–10. Fluorescence was restored in the presence of NO in CH₃OH/CH₂Cl₂ solutions of the compounds. Complexes 7, 8, and 10 exhibited a fluorescence response to NO in pH 7.0 or 9.0 buffered aqueous solutions. Spectroscopic studies revealed that NO-induced fluorescence enhancement in these Cu^{II} complexes occurs by reduction to Cu^I. The present studies demonstrate that Cu^{II} complexes are effective as fluorescent probes for detecting NO in both organic and aqueous environments.

Introduction

The discovery of nitric oxide (NO) as a biological signaling agent stimulated a wide range of research activities with the ultimate aim of elucidating the precise biological functions of NO.^{1–5} This goal is very challenging because NO is a highly reactive free radical. One critical mission of the research is to pinpoint the location of NO formation and NO-induced events at the cellular level. Thus, an indicator capable of visualizing NO in biological systems is desired, to provide selective and direct information about its production and migration with spatiotemporal resolution. A very promising approach for achieving this goal is the use of fluorescence methodologies.

An early small-molecule fluorescent probe for NO detection is *o*-diaminonaphthalene (DAN), which responds to the presence of NO oxidation products (e.g., NO₂[−], N₂O₃) with an increase in fluorescence intensity. As such, it can serve only as an indirect NO sensor.⁶ Moreover, DAN requires high-energy excitation for fluorescence imaging, which can

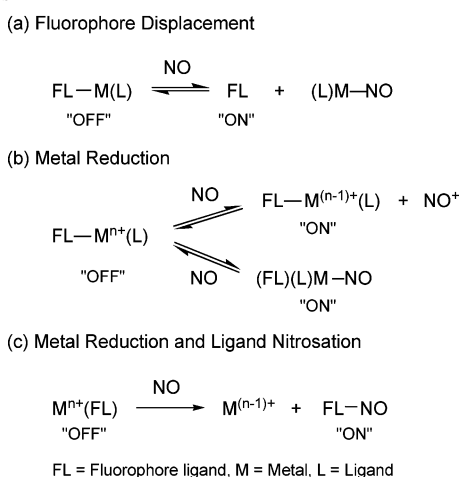
damage cells. To improve upon the properties of DAN, several *o*-diaminofluorescein compounds (DAFs) were prepared as fluorescent NO indicators. These compounds have been used for imaging NO in biological media, but the increased fluorescence of these compounds still requires an oxidized NO species. Like DAN, DAFs are also indirect NO sensors.^{6,7}

Our approach to obtaining a probe for detecting NO directly utilizes the chemistry of transition-metal complexes. Rapid interaction of a metal center with NO initiates subsequent chemistry, leading to the desired turn-on fluorescence emission. We have reported several metal complexes as fluorescent NO indicators following this strategy, including fluorophore displacement by NO from the metal center with concomitant fluorescence enhancement (Scheme 1a).^{6,8–13}

* To whom the correspondence should be addressed. E-mail: lippard@mit.edu.

- (1) Furchgott, R. F. *Angew. Chem., Int. Ed.* **1999**, *38*, 1870–1880.
- (2) Ignarro, L. J. *Angew. Chem., Int. Ed.* **1999**, *38*, 1882–1892.
- (3) Murad, F. *Angew. Chem., Int. Ed.* **1999**, *38*, 1856–1868.
- (4) Bon, C. L. M.; Garthwaite, J. *J. Neurosci.* **2003**, *23*, 1941–1948.
- (5) Pepicelli, O.; Raiteri, M.; Fedele, E. *Neurochem. Int.* **2004**, *45*, 787–797.

- (6) Hilderbrand, S. A.; Lim, M. H.; Lippard, S. J. In *Topics in Fluorescence Spectroscopy*; Geddes, C. D., Lakowicz, J. R., Eds.; Springer: New York, 2005; pp 163–188 and references cited therein.
- (7) Nagano, T.; Yoshimura, T. *Chem. Rev.* **2002**, *102*, 1235–1270 and references cited therein.
- (8) Franz, K. J.; Singh, N.; Lippard, S. J. *Angew. Chem., Int. Ed.* **2000**, *39*, 2120–2122.
- (9) Franz, K. J.; Singh, N.; Spingler, B.; Lippard, S. J. *Inorg. Chem.* **2000**, *39*, 4081–4092.
- (10) Hilderbrand, S. A.; Lim, M. H.; Lippard, S. J. *J. Am. Chem. Soc.* **2004**, *126*, 4972–4978.
- (11) Lim, M. H.; Lippard, S. J. *Inorg. Chem.* **2004**, *43*, 6366–6370.
- (12) Lim, M. H.; Kuang, C.; Lippard, S. J. *ChemBioChem* **2006**, web release date: June 21, 2006, DOI: 10.1002/cbic.200600042.
- (13) Hilderbrand, S. A.; Lippard, S. J. *Inorg. Chem.* **2004**, *43*, 5294–5301.

Scheme 1. Strategies of NO Detection Using Transition-Metal Complexes

Although this initial tactic allowed us to detect NO directly based on fluorescence with metal complexes, the chemistry was compatible only with organic solvents. In aqueous environments, H₂O molecules can replace the fluorophore ligand from the metal center, leading to fluorescence turn-on in the absence of NO. On the basis of these discoveries, we devised another strategy for NO detection, which involves reduction of a metal center by NO. NO reduction of a paramagnetic metal center to a diamagnetic state can restore the quenched fluorescence of a ligand fluorophore, which remains coordinated to the metal (Scheme 1b).^{14,15}

This chemistry is exemplified by reduction of a copper(II) dithiocarbamate complex to the Cu^I form with NO (Scheme 1b).¹⁶ The Cu^{II} phen or dmp complexes (phen = 1,10-phenanthroline; dmp = 2,9-dimethyl-1,10-phenanthroline) were reported similarly to react with NO in alcoholic and aqueous media to yield the corresponding Cu^I compounds (Scheme 1b).¹⁷ In the present work, aspects of which were previously reported in a preliminary form,¹⁴ we have utilized this chemistry to detect NO by preparing Cu^{II} complexes having a ligand with a dansyl or an anthracenyl group appended as a fluorophore. These complexes can detect NO by fluorescence turn-on in both organic and pH 7.0 or 9.0 buffered aqueous solutions. The only prior examples of fluorescent NO detection with Cu^{II} complexes occurred in aqueous methanol¹⁸ or in an aqueous pH 7.0 buffer and in cells,¹⁹ by a different mechanism, reduction of Cu^{II} by NO followed by dissociation of the N-nitrosated ligand (Scheme 1c). The Cu^{II}-based NO sensors presented here broaden the scope of metal coordination chemistry for NO detection.

Experimental Section

Materials and Procedures. All reagents were purchased from commercial suppliers and used as received unless stated otherwise. Dichloromethane (CH₂Cl₂) was purified by passage through alumina columns under an Ar atmosphere. Methanol, ethanol, and diethyl ether were used as received. Nitric oxide (NO; Matheson 99%) was purified by a method reported previously.¹⁰ NO was transferred to the reaction solutions by a gastight syringe in the glovebox. All NO reactions were performed under anaerobic conditions. Fluorescence emission spectra were recorded at 25.0 ± 0.2 or 37.0 ± 0.2 °C on a Hitachi F-3010 or a Photon Technology International fluorescence spectrophotometer. NMR spectra were obtained on a Varian 300 or 500 spectrometer, and IR spectra were recorded on an Avatar 360 FTIR instrument. Electron spray ionization mass spectrometry (ESI-MS) analyses were performed on an Agilent 1100 series instrument.

X-ray Crystallography. Suitable crystals were mounted in paratone N oil on the tips of glass capillaries and frozen under a -100 or -123 °C cold N₂ stream. Data were collected on a Bruker APEX CCD X-ray diffractometer with Mo K α radiation (λ = 0.710 73 Å) controlled by the SMART software package.²⁰ The general procedures used for data collection are reported elsewhere.²¹ Empirical absorption corrections were applied with the SADABS program.²² Data were processed using the SAINTPLUS and SHELXTL software packages.^{23,24} The structures were solved by direct methods. All non-H atoms were refined anisotropically. H atoms were assigned idealized positions and given a thermal parameter of 1.2 times the thermal parameter of the atoms to which they were attached. The structure solutions were checked for higher symmetry with PLATON.²⁵ In the structure of **9**, one dimethylformamide (DMF) and 0.5 CH₃OH solvent molecules are included. In the latter, a disordered C atom was refined isotropically. The highest electron density in the final difference Fourier maps for **9** was 1.215 e/Å³, in the vicinity of this disordered CH₃OH.

Electrochemistry. Cyclic voltammograms were recorded in an MBraun glovebox under N₂ with an EG&G model 263 potentiostat. A three-electrode setup was employed, consisting of a Ag/AgNO₃ reference electrode [0.01 M in CH₃CN with 0.5 M (Bu₄N)(PF₆)], a Pt mesh auxiliary electrode, and a Pt disk working electrode. The supporting electrolyte was 0.1 or 0.5 M (Bu₄N)(PF₆) in CH₃CN or CH₂Cl₂. Cyclic voltammograms were externally referenced to the Fc/Fc⁺ couple [conversions: Fc/Fc⁺ scale to NHE scale, Fc/Fc⁺ = +460 mV vs SCE with (Bu₄N)(PF₆) in CH₂Cl₂; SCE = +242 mV vs NHE].^{26,27}

Spectroelectrochemistry. A three-electrode setup was used consisting of a Ag/AgCl reference electrode, a Pt mesh working electrode, and a Pt wire auxiliary electrode. The supporting electrolyte was 0.1 M (Bu₄N)(PF₆) in CH₂Cl₂. The Cu sample solutions (0.2 mM) were prepared in air and purged with N₂ for 20 min before electrolysis in a 1-mm UV-vis cell containing the three electrodes.

- (14) Lim, M. H.; Lippard, S. J. *J. Am. Chem. Soc.* **2005**, *127*, 12170–12171.
- (15) Smith, R. C.; Tennyson, A. G.; Lim, M. H.; Lippard, S. J. *Org. Lett.* **2005**, *7*, 3573–3575.
- (16) Díaz, A.; Ortiz, M.; Sánchez, I.; Cao, R.; Mederos, A.; Sanchiz, J.; Brito, F. *J. Inorg. Biochem.* **2003**, *95*, 283–290.
- (17) Tran, D.; Skelton, B. W.; White, A. H.; Laverman, L. E.; Ford, P. C. *Inorg. Chem.* **1998**, *37*, 2505–2511.
- (18) Tsuge, K.; DeRosa, F.; Lim, M. D.; Ford, P. C. *J. Am. Chem. Soc.* **2004**, *126*, 6564–6565.
- (19) Lim, M. H.; Xu, D.; Lippard, S. J. *Nat. Chem. Biol.* **2006**, *2*, 375–380.

- (20) SMART: *Software for the CCD Detector System*, version 5.626; Bruker AXS: Madison, WI, 2000.
- (21) Kuzelka, J.; Mukhopadhyay, S.; Spingler, B.; Lippard, S. J. *Inorg. Chem.* **2004**, *43*, 1751–1761.
- (22) Sheldrick, G. M. *SADABS: Area-Detector Absorption Correction*; University of Göttingen: Göttingen, Germany, 1996.
- (23) SAINTPLUS: *Software for the CCD Detector System*, version 5.01; Bruker AXS: Madison, WI, 1998.
- (24) SHELXTL: *Program Library for Structure Solution and Molecular Graphics*, version 6.1; Bruker AXS: Madison, WI, 2001.
- (25) Spek, A. L. *PLATON, A Multipurpose Crystallographic Tool*; Utrecht University: Utrecht, The Netherlands, 2000.
- (26) Connelly, N. G.; Geiger, W. E. *Chem. Rev.* **1996**, *96*, 877–910.
- (27) Bard, A. J.; Faulkner, L. R. *Electrochemical Methods Fundamentals and Applications*; John Wiley & Sons: New York, 1980.

Optical spectra were obtained with a Spectral Instruments series 440 spectrophotometer with a continuously flowing current from a Bioanalytical Systems Model CV-50W potentiostat/galvanostat.

Syntheses. The ligand Ds-Hen [5-(dimethylamino)-*N*-(2-aminoethyl)-1-naphthalenesulfonamide, **2**] and its Cu complex [Cu(Ds-en)₂] (**7**) were prepared by previously reported methods.^{28,29} The syntheses of 5-(dimethylamino)-*N*-(2-pyridylmethyl)-1-naphthalenesulfonamide (Ds-HAMP, **3**), 5-(dimethylamino)-*N*-(8-quinolyl)-1-naphthalenesulfonamide (Ds-HAQ, **4**) and [Cu(Ds-AMP)₂] (**8**) are described elsewhere.^{12,14}

Potassium 4-(Anthracen-9-ylmethyl)piperazine-1-dithiocarbamate (AnCH₂pipCS₂K, **1).** A portion of 1-anthracen-9-ylmethylpiperazine·2HCl³⁰ (0.056 g, 0.16 mmol) was added to an aqueous solution of KOH (0.033 g, 0.59 mmol, 4.0 mL). The produced yellow solids were collected, dried in vacuo, and redissolved in diethyl ether (10 mL). Upon the addition of potassium hydroxide (9.0 mg, 0.16 mmol) and carbon disulfide (9.7 μL, 0.16 mmol) to the reaction solution, a pale-yellow precipitate immediately formed. The mixture was stirred overnight at room temperature. The solid was filtered, washed with Et₂O, and dried in vacuo (0.046 mmol, 0.12 mmol, 73%). Mp: 240–242 °C (dec). ¹H NMR (500 MHz, DMSO-*d*₆): δ (ppm) 2.46 (4H, t, *J* = 4.5 Hz), 4.24 (4H, s), 4.41 (2H, s), 7.51 (2H, t, *J* = 7.0 Hz), 7.56 (2H, t, *J* = 7.0 Hz), 8.08 (2H, *J* = 8.5 Hz), 8.50 (2H, d, *J* = 9.0 Hz), 8.57 (1H, s). ¹³C NMR (125 MHz, DMSO-*d*₆): δ (ppm) 213.7, 130.9, 130.9, 129.7, 128.8, 127.2, 125.8, 125.1, 125.0, 53.2, 53.0, 49.0. FTIR (KBr, cm⁻¹): 3082 (vw), 3051 (w), 3047 (vw), 2991 (w), 2923 (w), 2904 (w), 2857 (vw), 2857 (w), 2799 (w), 2766 (vw), 1624 (w), 1525 (w), 1493 (w), 1465 (m), 1454 (sh, vw), 1444 (m), 1411 (s), 1356 (w), 1338 (w), 1295 (w), 1273 (m), 1251 (m), 1213 (vs), 1182 (w), 1160 (vw), 1135 (m), 1118 (m), 1102 (w), 1026 (m), 1005 (w), 992 (m), 981 (m), 922 (s), 899 (vw), 881 (m), 866 (w), 857 (w), 836 (w), 802 (m), 774 (m), 774 (w), 756 (w), 727 (vs), 707 (w), 655 (w), 634 (w), 602 (w), 559 (w), 517 (w), 485 (w), 443 (vw), 417 (w). ESI(-)MS (*m/z*, [M - K]⁻). Calcd for C₂₀H₁₉N₂S₂, 351.1. Found: 351.5.

5-(Dimethylamino)-{3-[4-(3-aminopropyl)-piperazin-1-yl]propyl}-1-naphthalenesulfonamide (Ds-HAPP, **5).** To a CH₂Cl₂ solution (120 mL) of 3-[4-(3-aminopropyl)-piperazin-1-yl]propylamine (1.2 mL, 5.6 mmol) at 0 °C was added dropwise a CH₂Cl₂ solution (20 mL) of dansyl chloride (0.30 g, 1.1 mmol) over 1 h. The solution was allowed to warm slowly to room temperature as it was stirred overnight. A white solid was filtered, and the filtrate was collected. A pH 2.0 aqueous solution (50 mL) was added to the filtrate, and the aqueous layer was collected. The solution was adjusted to pH 11 by the addition of sodium hydroxide. The solution was extracted three times with CH₂Cl₂. Removal of the CH₂Cl₂ solvent gave a viscous yellow oil (0.32 g, 0.72 mmol, 65%). ¹H NMR (300 MHz, CD₃OD): δ (ppm) 1.45 (2H, q, *J* = 6.9 Hz), 1.60 (2H, q, *J* = 7.2 Hz), 2.03–2.40 (12H, m), 2.61 (2H, t, *J* = 6.9 Hz), 2.84–2.88 (8H, m), 7.25 (1H, d, *J* = 7.8 Hz), 7.52–7.59 (2H, m), 8.17 (1H, dd, *J* = 7.2 and 1.2 Hz), 8.31 (1H, d, *J* = 8.7 Hz), 8.53 (1H, d, *J* = 8.4 Hz). ¹³C NMR (125 MHz, CDCl₃): δ (ppm) 153.3, 137.1, 131.3, 131.2, 131.0, 130.5, 129.3, 124.5, 120.6, 116.5. FTIR (KBr, cm⁻¹): 3435 (br, m), 3064 (vw), 2941 (m), 2872 (w), 2811 (m), 2770 (m), 1612 (w), 1588 (m), 1575 (m), 1503

(w), 1474 (sh, w), 1462 (m), 1406 (w), 1392 (sh, w), 1369 (vw), 1353 (m), 1311 (s), 1269 (sh, vw), 1231 (w), 1201 (w), 1161 (sh, w), 1142 (vs), 1092 (w), 1072 (vw), 1059 (vw), 1043 (vw), 1008 (vw), 986 (vw), 971 (vw), 944 (w), 899 (vw), 836 (vw), 824 (vw), 791 (s), 740 (w), 682 (w), 623 (s), 571 (s), 499 (vw), 486 (vw), 461 (vw), 435 (vw). ESI(+)MS (*m/z*, [M + H]⁺). Calcd for C₂₂H₃₆N₅O₂S, 434.3. Found: 434.2.

[Cu(AnCH₂pipCS₂)₂] (6**).** A dark-brown solid was obtained from an aqueous solution (10 mL) of **1** (30 mg, 0.077 mmol) and copper(II) nitrate (8.9 mg, 0.038 mmol). The residue was filtered, washed with H₂O and Et₂O several times, and dried in vacuo (28 mg, 0.037 mmol, 97%). Mp: 260–262 °C. X-ray-quality crystals were obtained by vapor diffusion (CH₂Cl₂/Et₂O) at room temperature. FTIR (KBr, cm⁻¹): 3433 (br, w), 3080 (vw), 3048 (w), 2923 (w), 2900 (w), 2850 (w), 2801 (w), 2766 (w), 1622 (w), 1492 (s), 1434 (m), 1382 (vw), 1363 (w), 1336 (w), 1294 (w), 1274 (w), 1250 (vw), 1232 (vs), 1180 (vw), 1124 (w), 1093 (vw), 1019 (w), 989 (m), 946 (vw), 925 (vw), 886 (w), 864 (vw), 843 (vw), 801 (vw), 775 (vw), 730 (s), 706 (vw), 656 (vw), 635 (vw), 602 (vw), 590 (vw), 446 (vw), 430 (vw). Anal. Calcd for CuC₄₀H₃₈S₄N₄·0.5H₂O: C, 61.95; H, 5.07; N, 7.22. Found: C, 62.33; H, 5.09; N, 7.03.

[Cu(Ds-AQ)₂] (9**).** To a CH₃OH solution (5.0 mL) of **4**¹² (0.10 g, 0.26 mmol) was added a 0.1 M KOH solution (2.6 mL, 0.26 mmol). The solvent was evaporated under reduced pressure. The resulting residue was dissolved in CH₃OH (5.0 mL), and copper acetate (26 mg, 0.13 mmol) was added. The solution was refluxed for 6 h and slowly cooled to room temperature. A dark-brown solid was collected and washed with Et₂O (0.088 g, 0.11 mmol, 83%). Mp: 199–201 °C (dec). X-ray-quality brown crystals were obtained by vapor diffusion (DMF/Et₂O). FTIR (KBr, cm⁻¹): 3108 (w), 2988 (w), 2940 (w), 2866 (w), 2830 (w), 2787 (w), 1610 (w), 1578 (m), 1502 (vs), 1467 (m), 1382 (s), 1355 (w), 1322 (vs), 1296 (s), 1273 (w), 1239 (w), 1228 (w), 1189 (m), 1132 (vs), 1114 (w), 1090 (w), 1072 (w), 1060 (w), 1045 (w), 957 (m), 942 (m), 870 (m), 825 (m), 787 (s), 752 (w), 685 (w), 628 (s), 585 (s), 567 (m), 544 (w), 527 (w), 494 (w), 461 (vw). Anal. Calcd for CuC₄₂H₃₆S₂O₄N₆·H₂O: C, 60.45; H, 4.59; N, 10.07. Found: C, 59.99; H, 4.50; N, 9.98.

[Cu(Ds-APP)(OTf)] (10**).** A portion of **5** (50 mg, 0.12 mmol) was added to a CH₃OH solution (3.0 mL) of copper(II) triflate (42 mg, 0.12 mmol). The solution was stirred for 1 h, and volatile fractions were removed. The residues were dissolved in CH₂Cl₂ (5.0 mL), and a white solid was removed by filtration. Evaporation of the solvent from the filtrate provided a blue solid (67 mg, 0.10 mmol, 90%). Mp: 116–119 °C (dec). X-ray-quality blue crystals were obtained by vapor diffusion (CH₂Cl₂/Et₂O) at room temperature. FTIR (KBr, cm⁻¹): 3306 (w), 3258 (w), 2944 (w), 2873 (w), 2836 (vw), 2789 (w), 1610 (vw), 1590 (w), 1575 (w), 1500 (vw), 1461 (w), 1439 (vw), 1407 (w), 1391 (vw), 1352 (vw), 1287 (s), 1243 (s), 1225 (w), 1162 (m), 1146 (m), 1116 (w), 1090 (vw), 1070 (vw), 1062 (vw), 1029 (s), 965 (vw), 946 (vw), 928 (vw), 899 (vw), 839 (w), 792 (m), 760 (vw), 740 (vw), 683 (vw), 638 (s), 573 (m), 517 (m). Anal. Calcd for CuC₂₃H₃₄F₃N₅O₅S₂·2CH₂Cl₂: C, 36.84; H, 4.70; N, 8.59. Found: C, 37.09; H, 4.67; N, 8.73.

Results

Syntheses of Ligands. The ligand AnCH₂pipCS₂K (**1**; Figure 1) was prepared by the reaction of 1-anthracen-9-ylmethylpiperazine·2HCl³⁰ with carbon disulfide in the presence of a base. Bidentate ligands bearing dansyl groups

(28) Prodi, L.; Bolletta, F.; Montalti, M.; Zaccheroni, N. *Eur. J. Inorg. Chem.* **1999**, 455–460.

(29) Prodi, L.; Montalti, M.; Zaccheroni, N.; Dallavalle, F.; Folesani, G.; Lanfranchi, M.; Corradini, R.; Pagliari, S.; Marchelli, R. *Helv. Chim. Acta* **2001**, *84*, 690–706.

(30) Akkaya, E. U.; Huston, M. E.; Czarnik, A. W. *J. Am. Chem. Soc.* **1990**, *112*, 3590–3593.

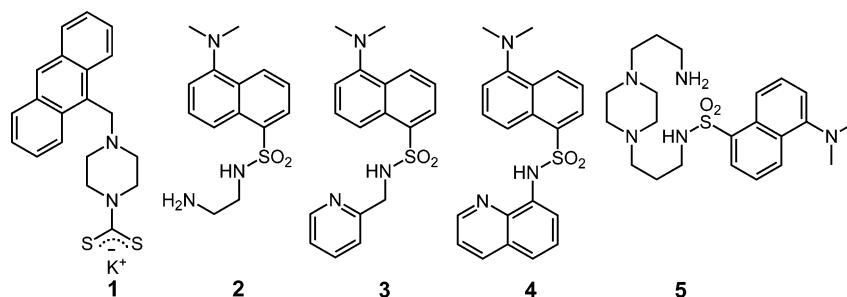


Figure 1. Chemical structures of AnCH₂pipCS₂K (**1**), Ds-Hen (**2**), Ds-HAMP (**3**), Ds-HAQ (**4**), and Ds-HAPP (**5**).

Table 1. Summary of X-ray Crystallographic Data

	6	9 -DMF·0.5CH ₃ OH	10
formula	C ₄₀ H ₃₈ CuN ₄ S ₄	C _{45.5} H ₄₅ CuN ₇ O _{5.5} S ₂	C ₂₃ H ₃₄ CuF ₃ N ₅ O ₅ S ₂
fw	766.52	905.54	645.24
space group	<i>P2₁/c</i>	<i>P2₁/n</i>	<i>P1</i>
<i>a</i> , Å	21.418(4)	13.851(7)	8.272(5)
<i>b</i> , Å	8.5585(17)	23.123(12)	12.900(7)
<i>c</i> , Å	10.154(2)	13.958(7)	13.942(8)
α, deg			84.277(10)
β, deg	102.08(3)	100.181(8)	84.374(9)
γ, deg			71.511(9)
<i>V</i> , Å ³	1820.1(6)	4400(4)	1400.4(14)
<i>Z</i>	2	4	2
ρ _{calc} , g/cm ³	1.399	1.367	1.530
cryst size (mm ³)	0.10 × 0.05 × 0.03	0.20 × 0.08 × 0.04	0.15 × 0.10 × 0.08
<i>T</i> , °C	−100	−100	−123
μ(Mo Kα), mm ^{−1}	0.865	0.646	0.992
θ limits, deg	1.94–25.50	1.76–25.03	1.47–25.50
total no. of data	13 611	38 868	10 731
no. of unique data	3395	7764	5150
no. of params	223	569	386
GOF ^a	1.147	1.098	1.080
R1 ^b	0.0739	0.0568	0.0434
wR2 ^c	0.1324	0.1462	0.1029
max, min peaks, e/Å ³	0.469, −0.494	1.215, −0.537	0.621, −0.300

^a GOF (goodness of fit based on F^2) = $\{\sum[w(F_o^2 - F_c^2)^2]/(m - n)\}^{1/2}$ (m = number of reflections; n = number of parameters refined). ^b R1 = $\sum||F_o| - |F_c||/\sum|F_o|$. ^c wR2 = $\sum\{w(F_o^2 - F_c^2)^2/\sum[w(F_o^2)^2]\}^{1/2}$.

(**2**–**4**) were obtained by reacting the amines and dansyl chloride according to previously reported procedures.^{12,14,28} A tetradentate ligand (**5**) was also obtained, which contains the dansyl group as a light-emitting unit (Figure 1). Slow addition of the precursor amine, 3-[4-(3-aminopropyl)-piperazin-1-yl]propylamine, to a solution of dansyl chloride over 1 h at 0 °C afforded the desired product **5** in moderate yield without further purification.

Synthesis and Structural Characterization of Cu Complexes. (a) [Cu(AnCH₂pipCS₂)₂] (**6**). The Cu complex **6** was prepared from an aqueous solution of Cu(NO₃)₂ and **1** in the ratio of 1:2. X-ray-quality brown crystals were obtained by vapor diffusion of Et₂O into a CH₂Cl₂ solution of **6**. The compound crystallizes in the monoclinic space group *P2₁/c* with $Z = 2$. Crystallographic data for **6** are summarized in Table 1, and the molecular structure with an atomic labeling scheme is shown in Figure 2. The Cu atom occupies a special position requiring a center of inversion and is coordinated by the four S atoms in a square-planar geometry. One of the two Cu–S distances, 2.2694(13) Å, is the shortest reported for copper dithiocarbamate complexes, which fall in the range of ~2.28 to ~2.32 Å.^{31,32} The C–S bond lengths, 1.713(5) and 1.715(5) Å, lie between the values of a C–S single bond, ~1.81 Å, and a C=S double bond, ~1.69 Å.^{31,33} Similarly, the C–N bond length, 1.323(6) Å,³³ has significant double-bond character, indicating delocalization of the π electrons

over the S₂CN moiety. Thus, the S₂CN groups are coplanar with the CuS₄ core. Selected bond lengths and angles are listed in Table 2 and are consistent with those of previously reported Cu analogues.^{31,32}

(b) [Cu(Ds-AQ)₂] (**9**) and [Cu(Ds-APP)(OTf)] (**10**). The Cu^{II} complex **9**, where Ds-AQ is the conjugate base of **4**,¹² was prepared from a CH₃OH solution of Cu(OAc)₂ and the appropriate ligand in a 1:2 ratio in the presence of a base, which is the same method as that used to prepare **8**.¹⁴ Dark-brown crystals of **9** were grown by vapor diffusion of Et₂O into a DMF solution. Crystallographic data for **9** are summarized in Table 1. The molecular structure with an atomic labeling scheme is presented in Figure 2, and selected bond lengths and angles are listed in Table 2. The Cu center in **9** is coordinated by four N atoms from two bidentate Ds-AQ ligands. The Cu–N_{amide} bonds [1.943(3) and 1.944(3) Å] are shorter than those of Cu–N_{quinoline} [1.993(3) and 2.001(3) Å] in the structure of **9**. The dihedral angle for **9**, Θ , measured between the planes of the two five-membered chelate rings, is 45.8°, indicating distorted tetrahedral Cu

(31) Mederos, A.; Cachapa, A.; Hernandez-Molina, R.; Teresa Armas, M.; Gili, P.; Sokolov, M.; Gonzalez-Platas, J.; Brito, F. *Inorg. Chem. Commun.* **2003**, *6*, 498–502.

(32) Jian, F.; Wang, Z.; Bai, Z.; You, X.; Fun, H.-K.; Chinnakali, K.; Razak, I. A. *Polyhedron* **1999**, *18*, 3401–3406.

(33) Greenwood, N. N.; Earnshaw, A. *Chemistry of the Elements*; Elsevier: New York, 1997.

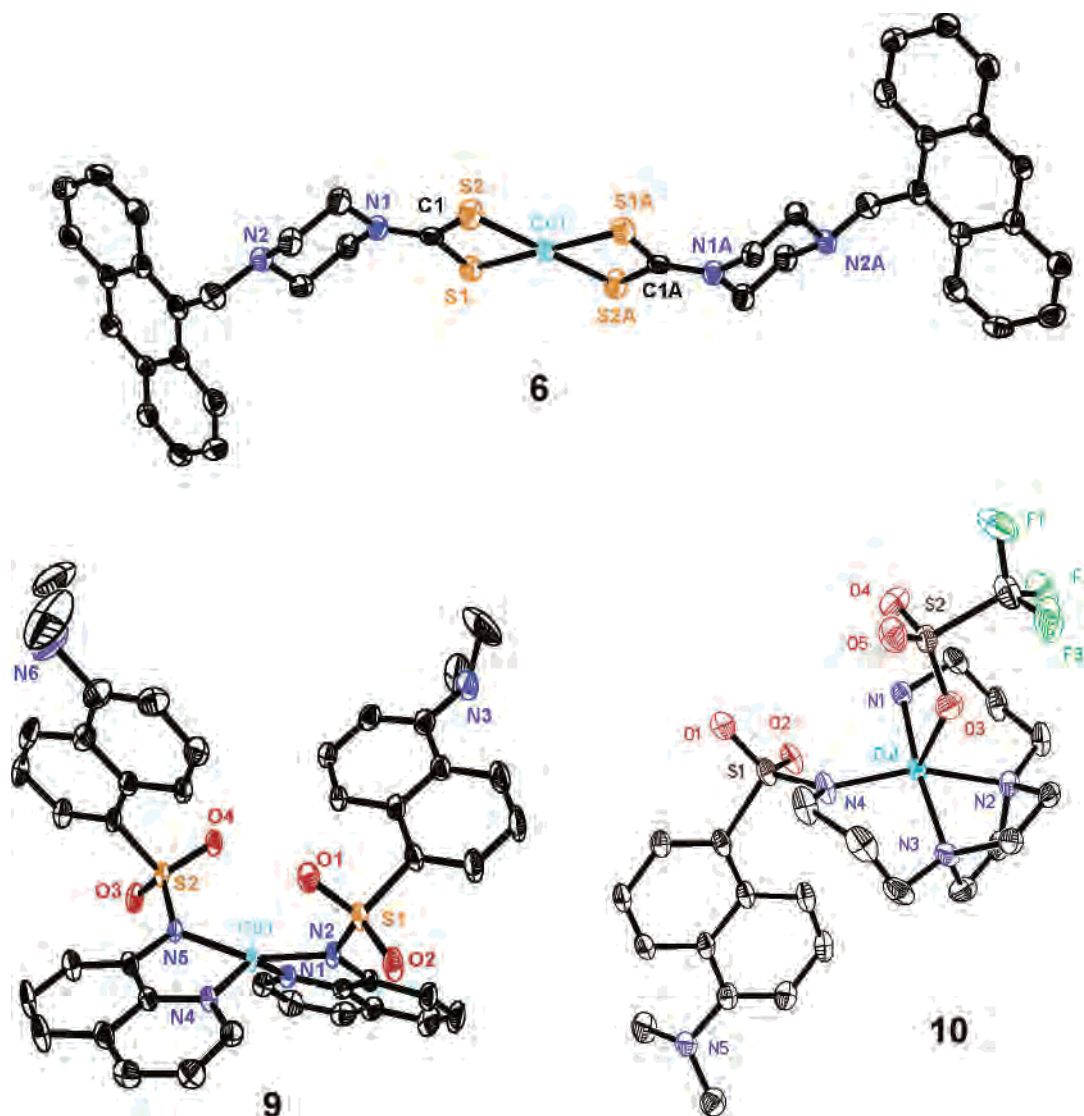


Figure 2. ORTEP diagrams of **6**, **9**, and **10** showing 50% probability thermal ellipsoids.

coordination geometry. Comparison of the dihedral angles of **7**,²⁹ **8**,¹⁴ and **9** ($\Theta = 3.9^\circ$, 39.3° , and 45.8°) suggests that the Cu complex **9** would be easier to reduce to a Cu^{I} species, anticipated as its NO reaction product, because it needs less reorganization than **7** and **8**. The bond lengths and angles of **9** are consistent with those of previously reported $[\text{Cu}(\text{qnsa})_2]$ ($\text{qnsa} = N$ -quinolin-8-yl-naphthalenesulfonamide).^{34,35}

Vapor diffusion of Et_2O into a CH_2Cl_2 solution of copper(II) triflate and **5** in a ratio of 1:1 produced blue X-ray-quality crystals of **10**. The molecular structure of **10** with an atomic labeling scheme is shown in Figure 2, and crystallographic data are summarized in Table 1. The Cu center is pentacoordinate with four N atoms from the tetradate Ds-APP ligand (Ds-APP is the conjugate base of **5**) and one O atom from a triflate anion arranged in an axially elongated square-pyramidal geometry. The bond lengths of Cu1-N1 , Cu1-N2 , Cu1-N3 , and Cu1-N4 are 1.983(3),

2.071(3), 2.028(3), and 1.987(3) Å, respectively. The Cu1-O3 distance is 2.364(2) Å, which is within the range of ~ 2.34 to ~ 2.53 Å for $\text{Cu}^{\text{II}}\text{OTf}$ in the Cambridge Structural Database (CSD version 5.27). The ratio of the two basal angles [$168.26(11)^\circ$ and $159.67(11)^\circ$] in a square-pyramidal structure, τ (an index of the degree of trigonality, 0.14),³⁶ is close to 0, indicating nearly idealized geometry. The Cu center lies slightly above the basal plane (0.26 Å). The bond lengths and angles within **10** are similar to those of previously published Cu complexes $[\text{Cu}(\text{bapp})(\text{Cl})]\text{Cl}$ and $[\text{Cu}(\text{bapp})(\text{ClO}_4)](\text{ClO}_4)$ [$\text{bapp} = 1,4$ -bis(3-aminopropyl)piperazine].³⁷ Selected bond lengths and angles are provided in Table 2.

Electrochemistry of Cu Complexes. The electrochemical behavior of **6** was studied by cyclic voltammetry in CH_2Cl_2 . The Cu complex **6** undergoes both a one-electron oxidation ($\text{Cu}^{\text{II/III}}$) and a one-electron reduction ($\text{Cu}^{\text{II/I}}$) at a Pt electrode, which is consistent with previously reported

(34) Congreve, A.; Katak, R.; Knell, M.; Parker, D.; Puschmann, H.; Senanayake, K.; Wylie, L. *New J. Chem.* **2003**, *27*, 98–106.

(35) Macías, B.; Villa, M. V.; García, I.; Castiñeiras, A.; Borrás, J.; Cejudo-Marin, R. *Inorg. Chim. Acta* **2003**, *342*, 241–246.

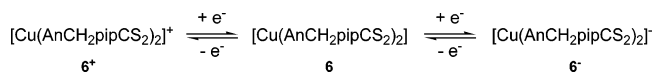
(36) Addison, A. W.; Rao, T. N.; Reedijk, J.; van Rijn, J.; Verschoor, G. C. *J. Chem. Soc., Dalton Trans.* **1984**, 1349–1355.

(37) Kwak, C.-H.; Jee, J.-E.; Pyo, M.; Kim, J.; van Eldik, R. *Inorg. Chim. Acta* **2004**, *357*, 2643–2649.

Table 2. Selected Bond Distances (Å) and Angles (deg)^a

Compound 6			
Cu1–S1	2.2694(13)	S1–Cu1–S2	77.68(5)
Cu1–S2	2.3008(14)	S1A–Cu1–S2	102.32(5)
S1–C1	1.713(5)	C1–S1–Cu1	84.90(16)
S2–C1	1.715(5)	C1–S2–Cu1	83.88(16)
N1–C1	1.323(6)	N1–C1–S1	123.0(4)
S1–Cu1–S1A	180.0(6)	N1–C1–S2	123.5(4)
		S1–C1–S2	113.4(3)
9·DMF·0.5CH ₃ OH			
Cu1–N1	1.993(3)	N1–Cu1–N4	146.48(13)
Cu1–N2	1.943(3)	N1–Cu1–N5	103.75(13)
Cu1–N4	2.001(3)	N2–Cu1–N4	102.16(13)
Cu1–N5	1.944(3)	N2–Cu1–N5	160.34(13)
N1–Cu1–N2	82.78(13)	N4–Cu1–N5	82.77(13)
		∠ ^b	45.8
Compound 10			
Cu1–N1	1.983(3)	N1–Cu1–N4	98.39(11)
Cu1–N2	2.071(3)	N2–Cu1–N3	73.20(11)
Cu1–N3	2.028(3)	N2–Cu1–N4	159.67(11)
Cu1–N4	1.987(3)	N3–Cu1–N4	90.66(11)
Cu1–O3	2.364(2)	O3–Cu1–N1	92.93(10)
N1–Cu1–N2	96.27(10)	O3–Cu1–N2	94.38(10)
N1–Cu1–N3	168.28(11)	O3–Cu1–N3	93.06(9)
		O3–Cu1–N4	98.84(10)

^a Numbers in parentheses are estimated standard deviations of the last significant figures. Atoms are labeled as indicated in Figure 2. ^b The angle ∠ is the dihedral angle between the planes of the two five-membered chelate rings.

Scheme 2. One-Electron Oxidation/Reduction of **6**

studies of copper dithiocarbamate complexes (Scheme 2).³⁸ A representative cyclic voltammogram of **6** is shown in Figure S1a (Supporting Information). A reversible oxidation at +0.10 V ($\Delta E_{p,p} = 0.083$ V) and a quasi-reversible reduction at -0.87 V ($\Delta E_{p,p} = 0.55$ V) were observed in CH₂Cl₂ (vs Fc/Fc⁺). Currents from both Cu^{II/III} and Cu^{II/I} processes, as shown in Figure S1 of the Supporting Information, are correlated linearly (i_{pc} and i_{pa} at $E_{1/2} = +0.10$ V; i_{pa} at $E_{1/2} = -0.87$ V) and not quite linearly (i_{pc} at $E_{1/2} = -0.87$ V) with (scan rate)^{1/2}.

The reduction potentials of **7–9** (vs Fc/Fc⁺) in CH₃CN for the Cu^{II}/Cu^I couple are -1.5 V (irrev),¹⁴ -0.82 V (rev, $\Delta E_{p,p} = 0.13$ V),¹⁴ and -0.70 V (rev, $\Delta E_{p,p} = 0.12$ V), respectively, confirming that **9** is more easily reduced than **7** and **8** (Figure S2 of the Supporting Information). This trend is predicted based on the above comparison of the dihedral angles in the crystal structures of **7–9**. The Cu^{II} complex **10** showed a reduction wave (Cu^{II}/Cu^I) vs Fc/Fc⁺ of -1.32 V in CH₂Cl₂ (Figure S2 of the Supporting Information).

Fluorescence Studies. (a) [Cu(AnCH₂pipCS₂)₂] (**6**). An initial fluorescence study of **6** indicated 3.1 (±0.3)-fold quenching in CH₂Cl₂/CH₃OH (1:1) relative to the free ligand (**1**) at an excitation wavelength of 370 nm (Figure 3a). Administration of excess NO (g) to a solution (CH₂Cl₂:CH₃OH, 1:1) of **6** resulted in a 5.5(±0.6)-fold fluorescence increase within 60 min (Figure 3b).

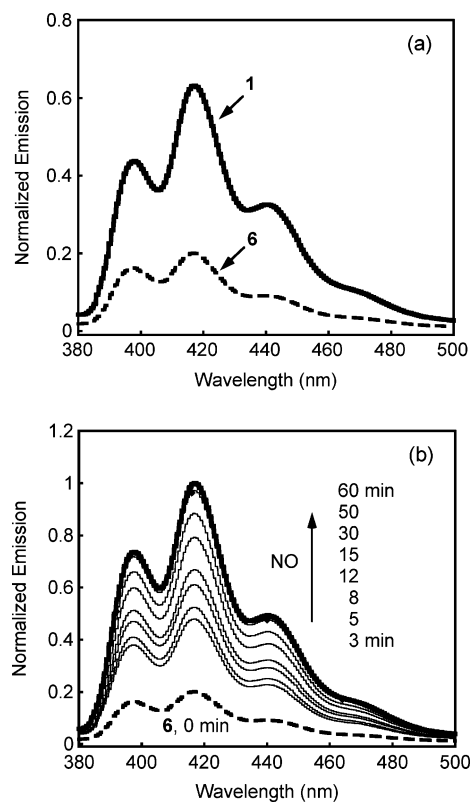


Figure 3. (a) Fluorescence emission spectra of **1** (20 μM, solid line) and **6** (20 μM, dashed line) in CH₃OH/CH₂Cl₂ (1:1; $\lambda_{ex} = 370$ nm). (b) Fluorescence response of **6** (dashed line, 0 min) upon the addition of 682 equiv of NO(g) (solid lines) at 3, 5, 8, 12, 15, 30, 50, and 60 min. The data here and in Figures 4–6 are reported as normalized emission spectra, a valid procedure for comparison purposes because in no case did Cu binding change the absorption intensity at the excitation wavelength by more than ±5%.

(b) [Cu(Ds-en)₂] (**7**), [Cu(Ds-AMP)₂] (**8**), [Cu(Ds-AQ)₂] (**9**), and [Cu(Ds-APP)(OTf)] (**10**). Coordination to Cu^{II} quenched the fluorescence of the ligands in solutions of **7–9**. A 31 (±2)-,¹⁴ 23 (±0.5)-,¹⁴ or 61 (±1)-fold decrease in fluorescence compared to that of the free ligands **2**, **3**, or **4** was observed in CH₃OH:CH₂Cl₂ solutions of **7**, **8**, or **9** (20 μM) (Figure 4). Upon the addition of 100 equiv of NO to CH₃OH solutions of **7–9**, the fluorescence of the **2–4** ligands was restored. The respective increases in integrated fluorescence were 6.1 (±0.2)-,¹⁴ 8.8 (±0.1)-,¹⁴ and 3.0 (±0.4)-fold, respectively, within less than 3 min (Figure 4). A 10 nM lower limit of NO detection for **8** was obtained by fluorescence measurements of solutions treated with decreasing concentrations of NO.¹⁴ Additional fluorescence measurements indicated that the H₂O-soluble Cu^{II} complexes **7** and **8** are capable of NO detection at pH 9.0 (50 mM CHES and 100 mM KCl).¹⁴ As shown in Figure 5, the quenched fluorescence of ligands **2** and **3** in complexes **7** and **8** was restored upon administration of NO, indicating that **7** and **8** are NO indicators with fluorescence turn-on in buffered aqueous as well as organic solutions. We also tested the fluorescence response of **8** to biologically relevant reductants such as ascorbic acid and glutathione because they might reduce Cu^{II} to Cu^I with fluorescence turn-on. As shown in Figure S3 of the Supporting Information, the quenched fluorescence of the fluorophore ligand **3** upon binding to Cu^{II}

(38) Hendrickson, A. R.; Ho, R. K. Y.; Martin, R. L. *Inorg. Chem.* **1974**, *13*, 1279–1281.

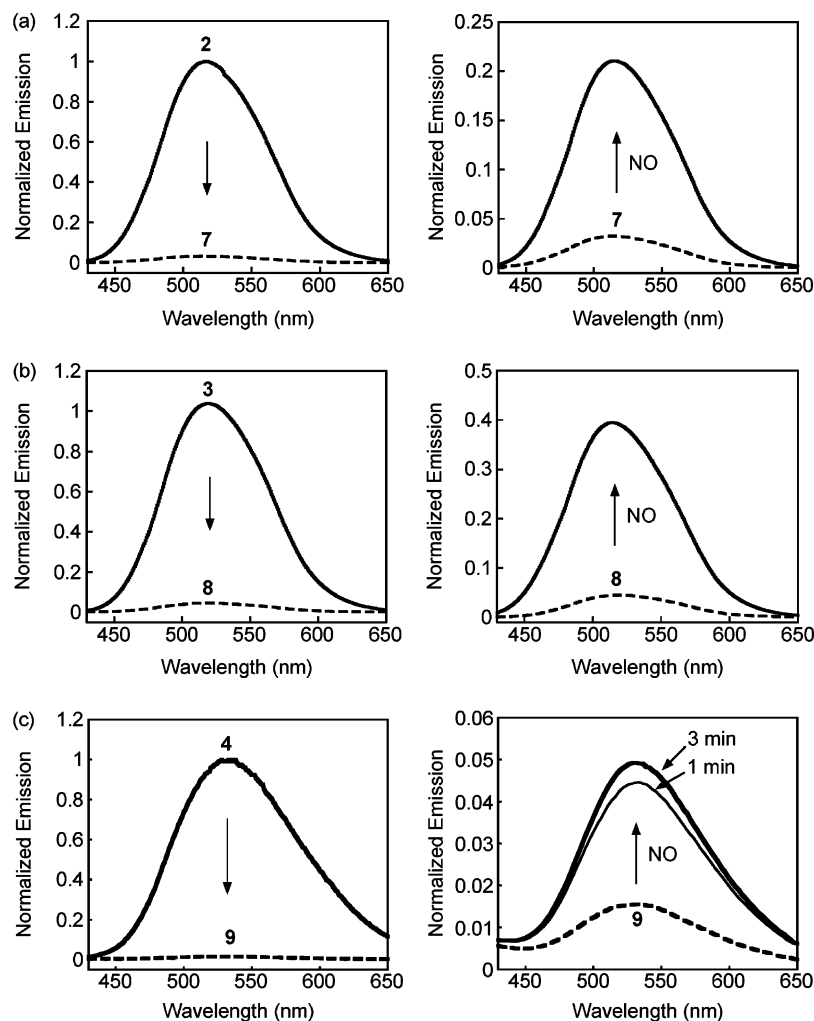


Figure 4. Left: emission spectra of **2** (a), **3** (b), and **4** (c) (40 μM , solid line) and **7** (a), **8** (b), and **9** (c) (20 μM , dashed line) in $\text{CH}_3\text{OH}/\text{CH}_2\text{Cl}_2$ (4:1) at 25 $^\circ\text{C}$. Right: emission spectra of **7** (a) and **8** (b)¹⁴ (20 μM , dashed line) upon immediate addition of 100 equiv of $\text{NO}(\text{g})$ (solid lines). (c) Fluorescence response of **9** (20 μM , dashed line) to 100 equiv of $\text{NO}(\text{g})$ (solid lines) at 1 and 3 min at 25 $^\circ\text{C}$ (right). Excitation wavelength, 342 nm.

was almost fully restored when 1 equiv of glutathione (or ascorbic acid, data not shown) was added to a solution of **8** in an aqueous buffer (50 mM CHES, pH. 9.0, and 100 mM KCl) under both anaerobic and aerobic conditions.

A CH_3OH solution of **10** (20 μM) displayed a 10 (± 0.6)-fold quenching in fluorescence, relative to the free ligand **5** (20 μM ; Figure 6a). The fluorescence was immediately increased by 2.3 (± 0.1)-fold after the addition of excess NO (Figure 6a). Moreover, **10** (10 μM) showed a 2.6 (± 0.2)-fold decrease in fluorescence in a pH 7.0 buffered solution (50 mM PIPES and 100 mM KCl), compared to the ligand **5** (Figure 6b). Upon the addition of excess NO , the fluorescence of **10** was enhanced by 1.6 (± 0.3)-fold over 10 min (Figure 6b). Although the fluorescence change is not large following the addition of NO to the pH 7.0 buffered solution of **10**, these observations suggest that a Cu complex containing dansyl fluorophore could be designed for NO detection at a physiological pH.

NO Reactivity of Cu Complexes. To investigate further the species responsible for the fluorescence enhancement upon the reaction of **6** with NO , spectroelectrochemical, IR, and fluorescence studies were carried out. The optical spectrum of a 20 μM solution of **6** in 1:1 $\text{CH}_2\text{Cl}_2/\text{CH}_3\text{OH}$

exhibited a decrease of the charge-transfer band ($\lambda_{\text{max}} = 436 \text{ nm}$; $\epsilon = 1.3 \times 10^4 \text{ M}^{-1} \text{ cm}^{-1}$) upon treatment with 682 equiv of added NO (Figure 7a), which suggests the formation of a Cu^{I} species. To help identify the nature of the NO -induced transformation, spectroelectrochemical studies were carried out. As shown in Figure S1 of the Supporting Information, a cyclic voltammogram of **6** reveals reversible oxidation and quasi-reversible reduction waves. Two potentials, +0.50 and -0.75 V (vs Ag/AgCl), were selected to generate Cu^{III} and Cu^{I} species electrolytically from the Cu^{II} complex **6**, and the process was monitored by UV-vis spectroscopy during electrolysis. Electrolysis at +0.50 V was accompanied by a change in the optical spectrum from that of **6** to that of $[\text{Cu}(\text{AnCH}_2\text{pipCS}_2)_2]^+$, with the maximum wavelength of the charge-transfer transition shifting from 436 to 428 nm (Figure 7b). In addition, the charge-transfer band of **6** at $\lambda_{\text{max}} = 436 \text{ nm}$ slowly disappeared upon reduction at -0.75 V (Figure 7c), which indicates the formation of a Cu^{I} . These spectroelectrochemical properties are similar to those of previously described copper dithiocarbamate complexes.³⁸

On the basis of these results, we conclude that a diamagnetic Cu^{I} species forms in the reaction of **6** with NO .

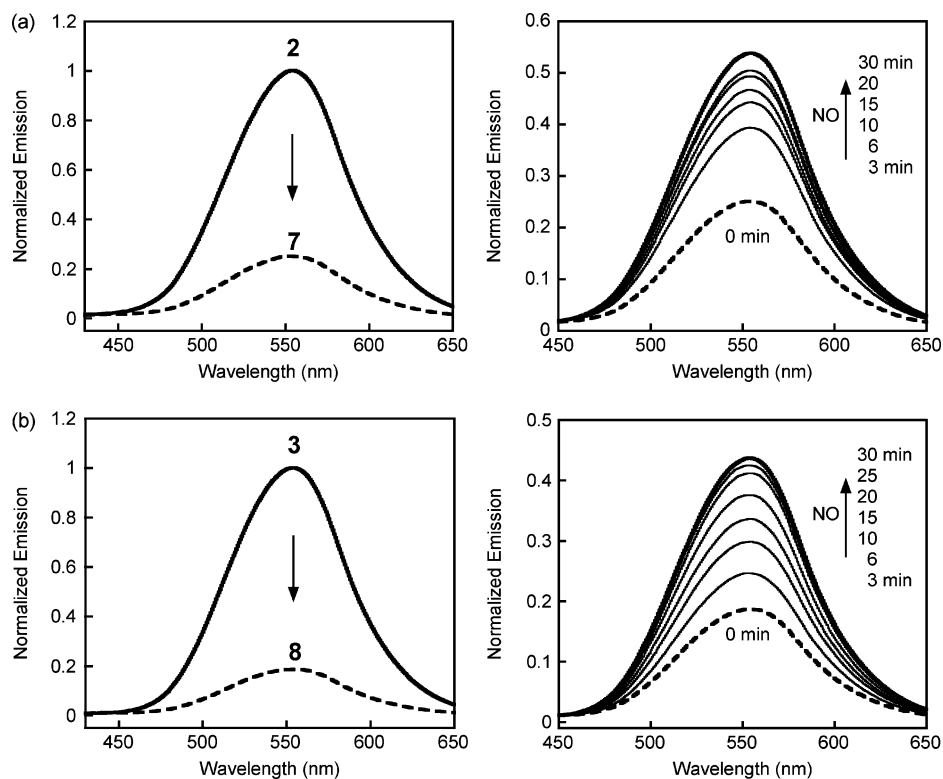


Figure 5. (a) Left: fluorescence emission spectra of **2** (20 μM , solid line) and **7** (10 μM , dashed line) at pH 9.0 (50 mM CHES and 100 mM KCl). Right: fluorescence response of **7** (10 μM , dashed line) to 100 equiv of NO(g) at 3, 6, 10, 15, 20, and 30 min (solid lines) at 37 $^{\circ}\text{C}$. (b) Left: emission spectra of **3** (20 μM , solid line) and **8** (10 μM , dashed line) in a pH 9.0 CHES buffered solution. Right: fluorescence response of **8** (10 μM , dashed line) to 100 equiv of NO(g) at 3, 6, 10, 15, 20, 25, and 30 min (solid lines) at 37 $^{\circ}\text{C}$.¹⁴ Excitation wavelength, 342 nm.

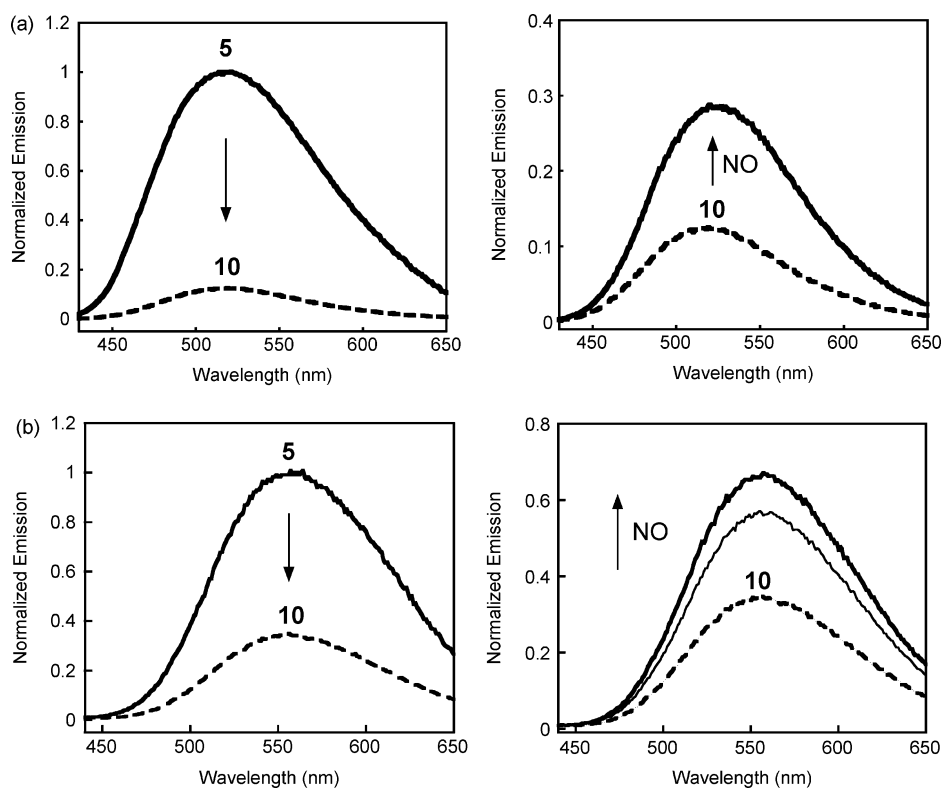


Figure 6. (a) Right: emission spectra of **5** (20 μM , solid line) and **10** (20 μM , dashed line) in CH_3OH at 25 $^{\circ}\text{C}$. Left: fluorescence response of **10** (20 μM , dashed line) to 682 equiv of NO(g) within 5 min (solid line) at 25 $^{\circ}\text{C}$. (b) Right: emission spectra of **5** (10 μM , solid line) and **10** (10 μM , dashed line) at pH 7.0 (50 mM PIPES, 100 mM KCl). Left: fluorescence response of **10** (10 μM , dashed line) to 682 equiv of NO(g) at 2 and 6 min (solid lines) at 37 $^{\circ}\text{C}$. Excitation wavelength, 342 nm.

Addition of $[\text{Cu}(\text{CH}_3\text{CN})_4](\text{BF}_4)$ to ligand **1** in a ratio of 1:2 produces fluorescence with the same intensity as that

measured in the reaction of NO with **6**, as shown in Figure S4 of the Supporting Information. This result lends further

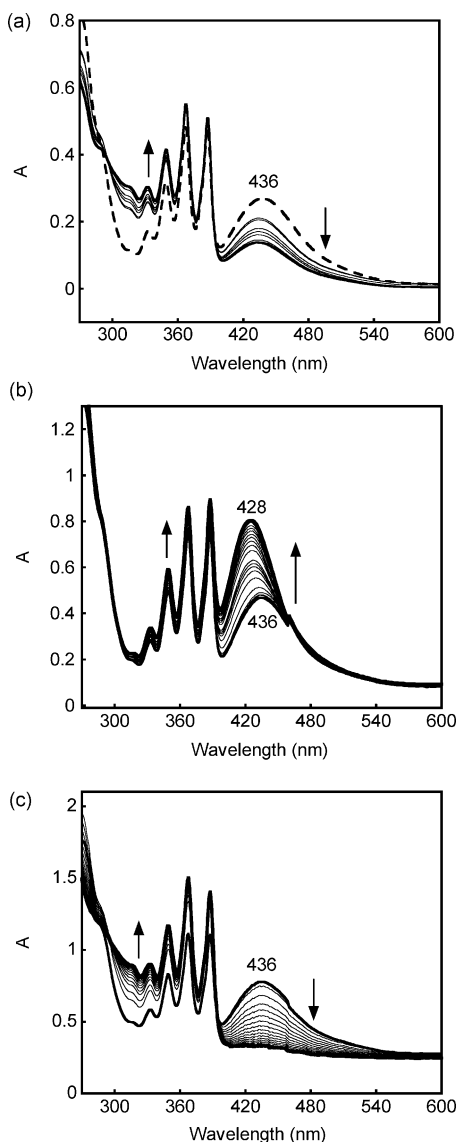
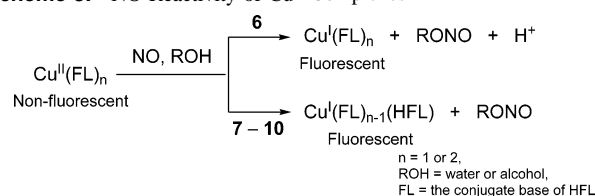


Figure 7. Optical spectra (a) from the reaction of **6** (20 μM) (dotted line) with 682 equiv of NO (solid line) over 60 min in $\text{CH}_2\text{Cl}_2/\text{CH}_3\text{OH}$ (1:1). Spectra of a solution of **6** (200 μM CH_2Cl_2 with 0.1 M $(\text{Bu}_4\text{N})(\text{PF}_6)$; 1-mm UV-vis cell) during oxidation (b) and reduction (c). The current at +0.50 V (b) or -0.75 V (c) with respect to the Ag/AgCl couple is continually provided as the optical spectra were collected for 40 min.

support to be proposed mechanism for the fluorescence enhancement accompanying the reaction of **6** with NO. The Cu^{I} species generated by reacting NO with **6** in $\text{CH}_3\text{OH}/\text{CH}_2\text{Cl}_2$ may exist in two different forms in solution: a copper nitrosyl adduct ($\text{Cu}^{\text{II}}-\cdot\text{NO} \leftrightarrow \text{Cu}^{\text{I}}-\text{NO}^+$) or a Cu^{I} compound having no bound nitrosyl. We can eliminate the former possibility by the absence of any IR band (KBr) in the 1600–1900- cm^{-1} region after completion of the reaction.^{16,39} Thus, introduction of NO reduces the Cu center, forming NO^+ , which can react with solvent CH_3OH molecules or possibly with ligand **1** at the S atoms of the dithiocarbamate moiety. No evidence for a nitrosothiol ($\text{RS}-\text{NO}$) or a thiol ($\text{RS}-\text{H}$) group was detected in the IR spectrum of the product ($\nu_{\text{S}-\text{O}} = 1400\text{--}1600\text{ cm}^{-1}$; $\nu_{\text{S}-\text{H}} = 2500\text{--}2600\text{ cm}^{-1}$),^{40,41} how-

Scheme 3. NO Reactivity of Cu^{II} Complexes



ever, suggesting either that it is not generated during the reaction or that its IR signature might overlap with other bands of the Cu complex. NO in the absence of CH_3OH did not enhance the fluorescence of **6** in the same manner as that occurring in the presence of the alcohol, which further supports our conclusion that the NO^+ cation, generated in the reaction of NO with **6**, nitrosates the CH_3OH solvent, forming a CH_3ONO species (Figure S5 of the Supporting Information). The reaction of **6** with NO would therefore appear to occur by reduction of Cu^{II} to Cu^{I} , forming NO^+ in solution, as shown in Scheme 3. This conclusion is consistent with previous studies of the reaction of Cu^{II} complexes $[\text{Cu}(\text{phen})_2]^{2+}$ and $[\text{Cu}(\text{dmp})_2]^{2+}$ with NO.¹⁷

An anticipated mechanism for the fluorescence enhancement of **7–10** by NO (Scheme 3) is that NO induces the formation of a diamagnetic Cu^{I} species with partial dissociation of the ligand fluorophore upon protonation by protons generated during the reaction. To investigate this possibility, the reaction of **8** with NO was examined in depth, the details of which were described previously.¹⁴ The reaction of **8** with NO as monitored by electron paramagnetic resonance (EPR), IR, and NMR spectroscopy involves reduction of Cu^{II} to Cu^{I} without complete release of the ligand fluorophore from the Cu center.¹⁴ Protonation of the sulfonamide functionality in **8** was readily observable by IR spectroscopy without overlapping another N–H functionality on the ligand (Figure 1).¹⁴

Discussion

Cu^{II} -based sensors are excellent compounds for detecting directly the presence of NO by fluorescence in a variety of contexts.⁴² In the present study, we examined anthracenyl and dansyl complexes, which display significant fluorescence turn-on in the presence of NO, demonstrating that these Cu^{II} -based probes are capable of its direct detection. Only Cu^{II} complexes **7**, **8**, and **10** were tested for a fluorescence NO response in aqueous media owing to the poor solubility of **6** and **9**. Compounds **7** and **8** could detect NO in pH 9.0 buffered solutions. At pH 7.0, ligands **2** and **3** bound to the Cu^{II} center become protonated at their sulfonamide functionalities and, consequently, there is no fluorescence quenching in **7** (10 μM) or **8** (10 μM) under these conditions.^{28,29} They, therefore, cannot be used to detect NO at a physiologically relevant pH. To improve the affinity of the fluorophore ligands for the Cu^{II} center, additional N donor atoms were introduced. As anticipated, the fluorescence of

(39) Park, S.-K.; Kurshev, V.; Luan, Z.; Lee, C. W.; Kevan, L. *Microporous Mesoporous Mater.* **2000**, *38*, 255–266.

(40) Williams, D. L. H. *Acc. Chem. Res.* **1999**, *32*, 869–876.

(41) Pavia, D. L.; Lampman, G. M.; Kriz, G. S. *Introduction to Spectroscopy*; Saunders College Publishing: Ft. Worth, TX, 1996.

(42) Lim, M. H.; Lippard, S. J. *Acc. Chem. Res.* **2006**, in press.

the Cu^{II} complex **10**, which incorporates the tetradentate ligand **5**, exhibits quenched fluorescence in both organic and pH 7.0 buffered solutions that is restored when NO is introduced. Although only a 1.6-fold fluorescence enhancement occurs upon treatment of **10** with NO, this observation demonstrates the potential utility of metal-based sensors for NO in biologically relevant media and contributed significantly to our development of even better NO sensors.¹⁹

NO detection occurs by the reduction of Cu^{II} in both the copper anthracenyl and dansyl systems. Spectroscopic studies revealed that NO reduces Cu^{II}, forming NO⁺. The resultant Cu^I species is responsible for the fluorescence increase in the NO reaction. Ligands such as **1** and **3** are fluorescent in the presence of [Cu(CH₃CN)₄](BF₄) but not Cu^{II} salts. Although, we were unable to characterize the Cu^I species by X-ray structural analyses, IR studies showed no formation of copper nitrosyl complexes during the NO reactions. We can, therefore, rule out Cu–NO compounds as the species responsible for the fluorescence turn-on in the present work. Because a protic solvent is required for the NO-induced fluorescence increase, we propose that the nitrosonium ion formed during the reaction reacts with the solvent molecules, CH₃OH or H₂O, driving the formation of fluorescent species and the final Cu^I compound (Scheme 3).¹⁷ Thus, introduction of NO may cause fluorescence enhancement of the Cu complexes via reduction followed by the formation of NO⁺, which, in turn, reacts with solvent molecules such as CH₃OH and H₂O. The intracellular reductants glutathione and ascorbic acid can also induce a fluorescence response from Cu complexes in this class (Figure S3 of the Supporting Information). The likely instability of the Cu^I species formed under aerobic conditions and the nearly full restoration of the ligand fluorescence in the reaction of **8** with glutathione suggest that the species responsible for the fluorescence enhancement is the free ligand. Thus, the underlying chemistry may occur by a mechanism, distinct from that of the NO reaction, involving displacement of the ligand

fluorophore by the reductant. This result emphasizes that successful application of NO-induced fluorescence enhancement involving Cu redox chemistry in living cells requires a complex that is not activated for light emission by cellular components in the absence of NO.¹⁹

Summary

Five Cu^{II} complexes (**6–10**) were synthesized and characterized as fluorescent NO sensors. Cu^{II}-induced fluorescence quenching was observed in all five compounds compared to that of the free ligands. A significant turn-on emission was observed upon the addition of NO(g) to an organic or aqueous solution of all of the Cu^{II} complexes. Significantly, **7**, **8**, and **10** exhibited a fluorescence increase in a pH 7.0 or 9.0 buffered aqueous solution upon treatment with NO. Mechanistic studies indicate that the fluorescence enhancement is basically caused by NO-triggered Cu^{II} reduction and generation of a diamagnetic Cu^I species. This work demonstrates that Cu^{II} complexes can function as fluorescence-based turn-on NO sensors in both organic and aqueous environments. This discovery forms the foundation for developing metal-based probes for NO detection in biological systems.

Acknowledgment. This work was supported by the National Science Foundation. The NMR spectrometer was funded through NSF Grant CHE-9808061. M.H.L. is grateful to the Martin Family Society for partial support. We thank Professor Daniel G. Nocera and Joel Rosenthal for assistance with the spectroelectrochemistry experiments of compound **6**.

Supporting Information Available: X-ray crystallographic data in CIF format of compounds **6**, **9**, **10**, and figures of cyclic voltammograms of compounds **6**, **9**, **10**, and fluorescence response and spectra of compounds **6** and **8**. This material is available free of charge via the Internet at <http://pubs.acs.org>.

IC0609913